DESIGNING A HARDWARE-IN-THE-LOOP SIMULATION TEST BED FOR AIRCRAFT ENERGY MANAGEMENT APPLICATIONS

Alessandro Dell'Amico[1,2]

[1]Saab AB
[2]Linköping University

Abstract

This paper outlines the design and implementation of a full-scale flexible test rig, an Iron Bird, for research and evaluation of energy management strategies for aircraft applications. Electrification increasingly takes a larger part of the on-board system design as seen in both the civil and military sector. As the need for more electric power and cooling capability increases, consequently, efficient means to also manage the energy and power are necessary. The test rig allows a full hardware-in-the-loop simulation of a complete flight mission of a generic aircraft where both hardware, power emulation, and software models are integrated. The paper presents the design aspects, control strategies, and a complete simulation of a generic fighter aircraft mission to prove the usefulness of the test rig.

Keywords: Energy management, more electric aircraft, hardware-in-the-loop simulation, iron bird

1. Introduction

A higher degree of electrification of on-board aircraft systems requires an increased electric power generation and cooling capability. This is seen in both the civil and military sector where flight control actuation, environmental control systems, de-icing systems, and even propulsion in some cases, are design alternatives to the traditional counterparts, [1], [2], [3]. This comes with an expectation on improving aircraft performance while decreasing operational and maintenance cost. While electrifying secondary systems drives the electric power need, the military sector also predicts an increased power need for sensors and even weapons. Managing the power and energy in an efficient way will be crucial to optimize mission performance or reduce fuel consumption. Early testing of control strategies, design alternatives, and integration aspects facilitates the transition. A hardware-in-the-loop simulation test rig, an Iron Bird, is developed for research and development purposes of energy management applications in a collaboration between Saab AB and Linköping University. A complete aircraft can be implemented where the flight controls, electric power and distribution, hydraulics, and emulated loads exist as hardware while the rest of the systems, including a flight simulator, exist as software. Emulating different electric loads allows a flexible test rig where different systems' characteristics can be emulated and interact with the flight controls and supply systems. The distribution system monitors all outgoing channels in real-time. The information is collected and sent to the energy management system whereupon different strategies are evaluated in terms of efficiency and complexity.

A potential benefit from electrifying aircraft systems is the adoption of one power source, which would open to more advanced energy management strategies. According to [4] energy management are methods to controls all energy flows and systems that contain energy storages, while power management refers to the instantaneous power generation and distribution where typically energy storages are not considered. Energy, or power management, is not only about managing the energy flow, but also to find a balanced and optimal system architecture considering all energy forms (electrical, hydraulic, pneumatic, mechanical) considering the mission objectives, [5]. This includes: power generation, transformation, distribution, consumption. Regarding control and managing the energy flow,

the typical approach today is electrical load management that utilizes load shedding according to a priority scheme if the consumed power is greater than the available, which can occur in certain flight phases or during an emergency, [4]. More advanced strategies looks at more dynamic approaches, e.g. source management controls multiple sources in such a way to minimize power losses, or to use energy storages to reduce power peaks, or utilizing power sharing of slow responding loads. An approach to using energy storages on-board, besides from supplying emergency power or during engine start, is to provide additional power if the total need exceeds the generator capacity, [6]. This approach could help down-sizing the main power generation system. An alternative to battery as energy storage are supercapacitors, that can provide the required peak power for highly dynamic loads, such as actuators, to reduce the load on the generation system and finally the engine, [7]. The generation system could be optimized considering the consumers actual load, and not the maximum load, where appropriate, [8]. An energy management system would then be required to avoid overloading the system.

An Iron Bird is typically a test rig replicating critical systems of an aircraft, usually the flight control, landing gear, and hydraulics, [9], [10]. The main purpose being to minimize development risk and provide integrated testing before flight, as well as unloading ground and flight testing. A modular approach to an Iron Bird adapts to different actuators and layouts, the simulated aerodynamic loads are chosen according to the test, and different test can be planned, including the flight mission and manoeuvres, [11]. Of particular focus for the work in this paper are studies on hydraulic and electric actuation systems. The two most common solutions today for electrification of the actuation system are the electrohydrostatic actuator, EHA, and the electromechanical actuator, EMA, [12], [13]. The electric actuators are an energy efficient solution compared to hydraulic actuators, but there are concerns regarding weight, size, and safety, when it comes to high performance aircraft. The power and thermal characteristics differ to the hydraulic actuators and depend on the actuator loading. One of the most critical system of the Iron Bird is the air load simulation system, the capability to dynamically apply the actuator loads based on a flight profile, [14], [15], [16]. This is an electrohydraulic system that needs to be controlled in such manner that the closed loop response greatly exceeds the one of the test object.

The focus of this paper is the development of a generic and flexible Iron Bird for research purposes. The paper describes the design process, the implementation of all interacting systems and necessary control strategies and models. A demonstration of a complete flight mission of a generic fighter aircraft validates the Iron Bird's functionality.

2. System description

The Iron Bird is depicted in figure 1. This is an Iron Bird donated to Linköping University by Saab AB when it was decommissioned. Originally the rig consisted of two elevators and rudder control surfaces, the hydraulic actuation and supply systems, and the flight control computers. The hardware in place was originally specified for transport aviation, however, since 2017, the Iron Bird has been gradually modified and new systems added to increase its functionality, enable more flexibility, and evaluate new technology. Today it is a test rig strictly for research purposes that allows for hardware-in-the-loop simulation of different aircraft system architectures and energy management strategies through the integration of a flight simulator. The purpose of the test rig is to be generic. Any aircraft can be represented to some extent through the selection of proper models and control strategies. Although the components are specific, scaling the control surface moments to the physical actuators stall loads means that they experience the same relative load as the modelled actuator.

2.1 Iron Bird HWIL strategy and architecture

The Iron Bird's architecture is illustrated in figure 2. The flight simulator is configured for the intended aircraft configuration and flight mission. A model of the aircraft on-board systems is derived and integrated with the flight simulator. To which extent the on-board systems architecture is representative depends on the specific use case. The models are implemented in the real-time system that communicates with the hardware through dedicated IO. The hardware consists of the electric power supply and distribution system, the flight control system, the hydraulic power supply system, and electric

Figure 1 – The Iron Bird test rig at Linköping University.

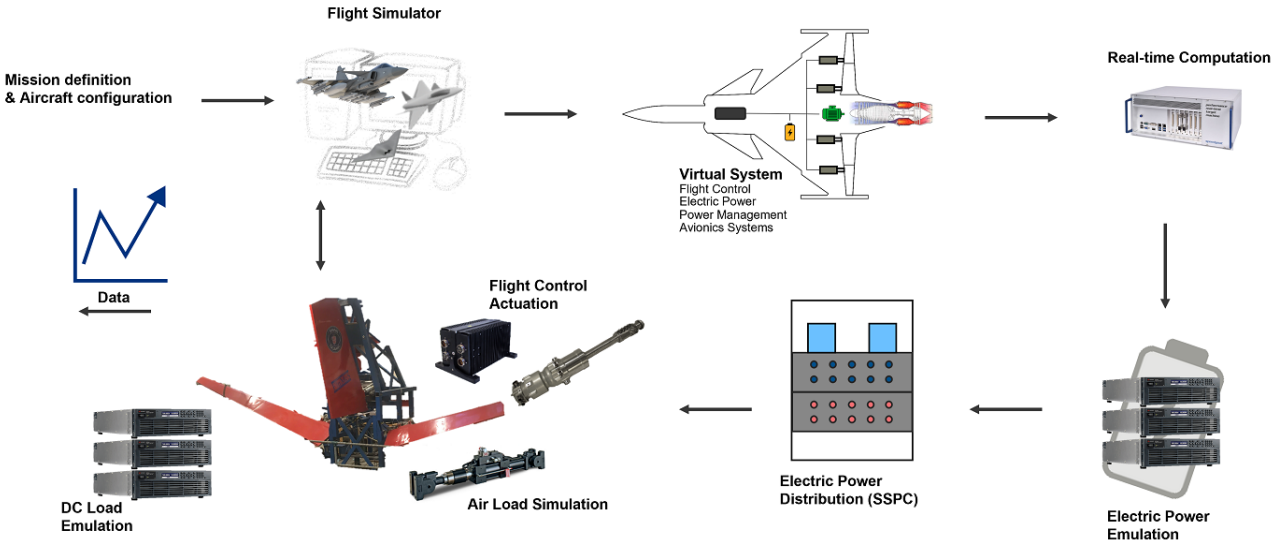

Figure 2 – The Iron Bird overall architecture. The shown actuator is only for illustrative purpose.

loads. The required signals for the flight simulator are sampled and fed to respective model to close the loop.

2.2 Hardware system

The Iron Bird was modified to host five control surfaces, four horizontal and one vertical. This facilitates a larger test scope where actuators not only can be individually evaluated but also the interaction of several units together with the supply system. Two EMAs are installed on the outer control surfaces and two SHAs on the inner horizontal control surfaces and rudder. The EMA is a direct driven ball-screw actuator. It has dual redundant motor with a single ball-screw and is supplied from two separated 270 VDC systems for high power supply, and two 28 VDC systems for low power supply. The dedicated control unit handles all control and monitoring and takes commanded actuator position as input.

The SHA are two hydraulic actuators in parallel, as shown in figure 3. A separate flight control computer handles the loop closure and monitoring. The EMA and SHA have similar stall load capacity

but for practical reasons during installation the EMA has twice the hinge arm length than the SHA, 0.16 m compared to 0.08 m.

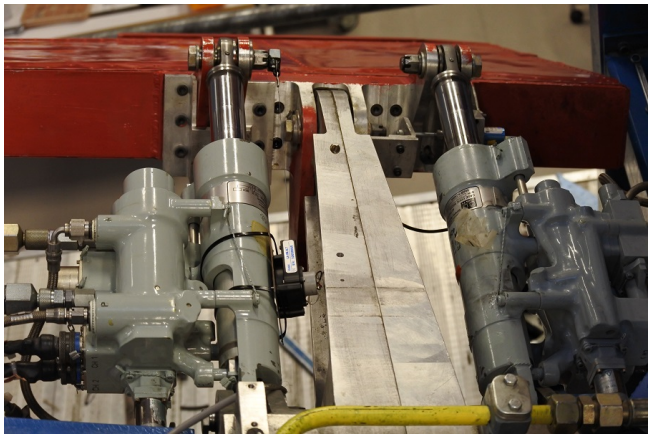

Figure 3 – The dual redundant servohydraulic actuator

The flight control actuators are subjected to an external load through an air load simulation system. This is a closed loop force control system with much faster response than the flight actuator. The purpose is to replicate the hinge moment due to the aerodynamic loads during flight by applying a linear force through an opposite hinge arm to the flight actuator, attached to the same point on the control surface. The reference force to the control loop is defined from the flight simulator's aerodynamic model that calculates the hinge moment depending on the flight condition and control surface deflection. The measured control surface deflection is measured and send back to the flight simulator. The details on the air load system are subject to a future publication and will not be detailed here. Figure 4 shows how the air load system is installed to the EMA.

Figure 4 – The EMA with air load actuator below. The EMA is masked due to confidentiality reasons.

The hydraulic supply system is a commercial off-the shelf electric servo motor driven fixed displacement pump shown in figure 5. The motor and inverter are from Baumüller and the pump from Voith. The package has a rated power at 23 kW and the pump can deliver up to 56.9 l/min at a speed of 3600 rpm. Although supplied from 400 VAC it is also possible to feed the inverter's DC line directly from a DC source. Two equal units are used: one for the hydraulic flight actuation system, one for the air load system. The hydraulic supply pressure is controlled by the electric motor's inverter in a closed loop. It is set at 300 bar for the air load system and 210 bar for the flight actuation system. An accumulator at 4 litres is installed for the air load system to cover any instant flow demand. A small accumulator at one litre is installed for the flight actuation system. Only one unit is installed for the flight actuation system due to cost restrictions. Since the servo drive has a very high response, the system can emulate a traditional hydraulic supply system where the pump is driven directly by the

engine shaft through the gearbox or emulate the more modern solution with a local electro-hydraulic power pack.

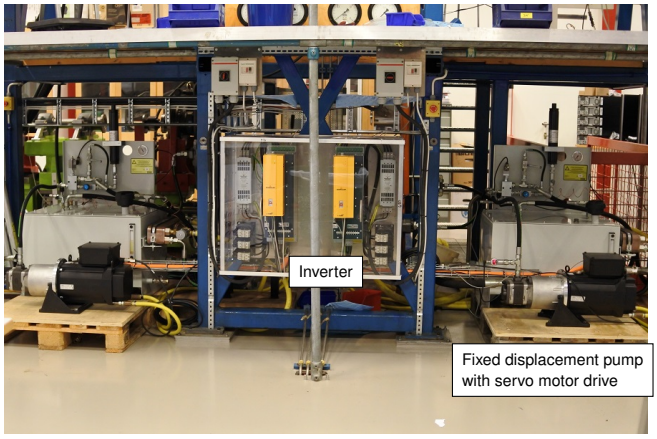

Figure 5 – The two hydraulic supply units.

The electric power and distribution system is shown in figure 6. The main power generation consists of Keysight RP7972 20 kW units and are set to deliver 270 VDC. There are two sides in order to emulate a redundant system and make the Iron Bird future proof. A similar units, but smaller at 5 kW, are used as DC loads. In practice all units can be used as either supply or loads which makes the set up flexible. The units are fully programmable where either the supply voltage or current draw are changed during the flight simulation. An update signal can be sent every 5 ms. The strategy is to command each unit according to static models that predict the voltage or current characteristics. The units allow to change the internal control loop's bandwidth which is defined in order to emulate the desired behaviour of the system. There is also an in-built pre-filter that shapes the command signal. The main power is connected to the distribution unit which demonstrates solid-state technology. It fulfils the purpose of distributing the main power to each load and safety disconnect is case of failures such as over-current. Each channel's current level is monitored and sent to the flight management system. The main power is also switched and distributed to 28 VDC.

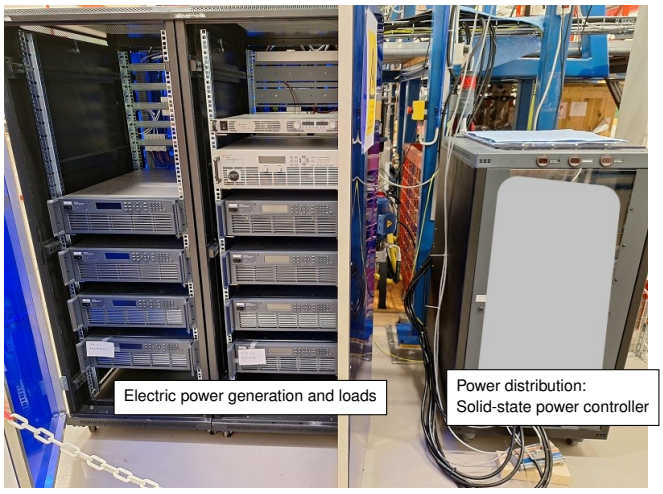

Figure 6 – The electric power and distribution system. The photo is partially masked due to confidentiality reasons.

The real-time system is the *Performance Real-Time Target Machine* from *Speedgoat* with several dedicated IOs for analog, digital and serial communication with hardware. Several signal are monitored: actuator position, actuator load force and pressure, actuator supply current, DC load current, actuator temperature (motor winding and controller).
The rig's hardware architecture is illustrated in figure 7 and shows how the components are connected.

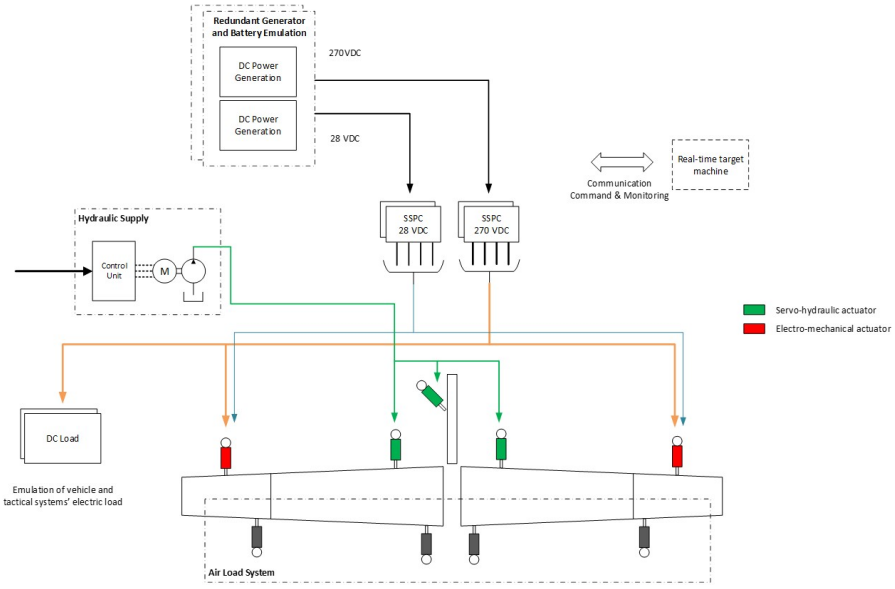

Figure 7 – Illustration of the rig's hardware architecture.

2.3 Software system

The software architecture is illustrated in figure 8. A graphical user interface let's the user interact with the systems during run time. The virtual model consists of the flight simulator, the hydraulic and electric supply systems, the actuation system, the vehicle systems, the tactical systems, and the flight management system. The virtual model communicates with the hardware through the dedicated IO. The actuator commands from the flight control laws are sent through the analogue and serial interface to the hydraulic and electric actuators respectively. The actual actuator position are sent back through the IO to the flight simulator to give the control surface deflection. The deflection is used both by the 6-DOF aircraft model and the hinge moment calculation. The calculated hinge moments are sent to the load actuation system. The vehicle and mission systems model calculate the current draw for each system. The commanded current draw is sent to the DC load emulation system through the Ethernet interface. A safety function monitors any deviation from the expected behaviour. For example, if the actuated load is higher than expected, the load system's by-pass valve is activated to disconnect the load from the flight actuator. The time-step has been carefully selected for each software component. The base frequency is at 10 kHz and is defined by the air-load system. All other models use a slower sampling time where possible in order to reduce the computational burden.

3. Case study

A fictive and simplified case study is defined to highlight the intended use of the Iron Bird. Only a few subsystems are included and safety or any proper sizing is not considered. A virtual model is developed and implemented in the real-time system and interfaces with the hardware. It include various loads to highlight different behaviour of the systems during flight. A flight mission is configured where the flight simulator, supply systems, actuation and vehicle systems, and mission systems interact. The models are to a large extent implemented using the *Simscape* package in *Matlab/Simulink*.

3.1 Aircraft system definition and modelling

The overall system architecture is illustrated in figure 9. The engine provides thrust to the aircraft and mechanical power and rotational speed to the gearbox, where two generators and two hydraulic pumps are attached (dual for redundancy reasons). The electric system provides 270 VDC and the hydraulic system 28 MPa hydraulic pressure. The low voltage 28 VDC is not modelled but required in the actual rig. The flight actuation systems considers the primary control surfaces: inner and outer elevons, canards, rudder. The outer elevons are equipped with dual redundant electromechanical actuators and the other control surfaces with dual redundant servohydraulic actuators. The inner elevons have a stall load of 115 kN, the outer and canards 85 kN, and the rudder 50 kN. An electric

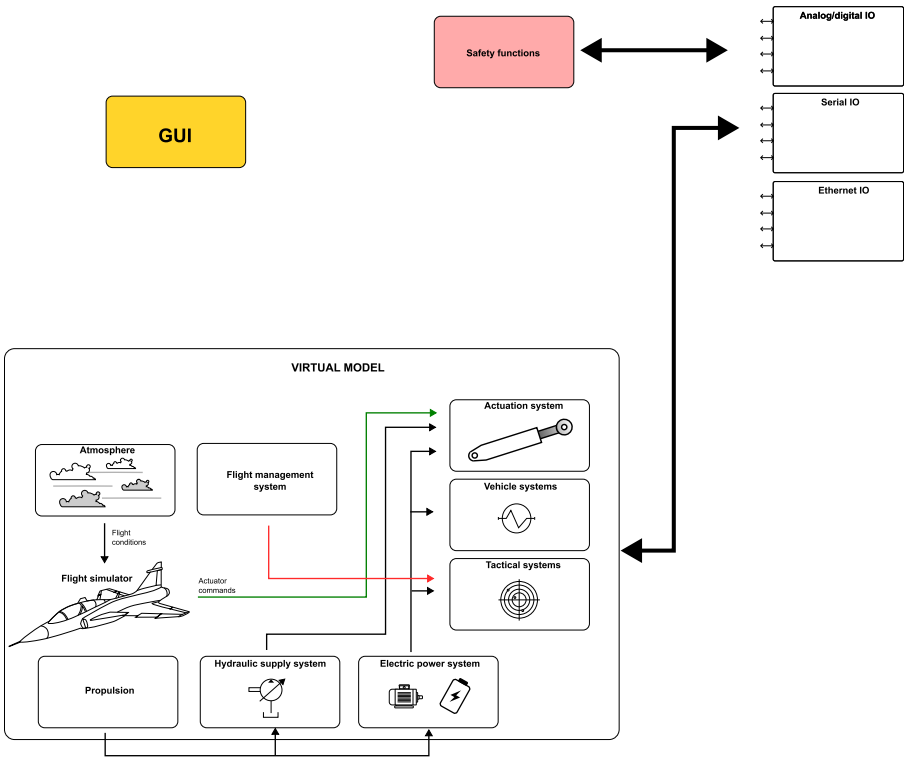

Figure 8 – Illustration of the rig's software architecture.

fuel pump is integrated to provide a boost of the fuel supply when the after burner is activated, with a maximum power of 10 kW. The mission systems consist of a radar and electronic warfare system with a maximum power of 10 kW each. All electric loads are connected to either 270 VDC system.

3.1.1 Aircraft model

The aircraft is a 6-DOF model of a delta-canard fighter, described in detail in [17]. The general data is listed in table 1. The model includes the aerodynamic forces and moments, control surface hinge moments, propulsion with thrust, and the flight control laws. An atmospheric model provides the reference temperature and pressure at specific flight altitude.

Parameter	Value	Unit
Wing area	45	m^2
Wing span	10	m
Wing chord (mean)	5.2	m
Mass	9100	kg
Ix	21000	kgm^2
Iy	81000	kgm^2
Iz	101000	kgm^2
Ixz	2500	kgm^2

Table 1 – Aircraft configuration parameters.

3.2 Propulsion and fuel system

An additional motor component is modelled that provides the shaft rotational speed and max power off-take. It takes the flight altitude, Mach number, ISA deviation, and thrust setting as input. The maximal settings are defined to 17000 rpm and 250 kW. Figure 10 shows an example how the speed and maximum power-off take varies with thrust setting at 10 km and Mach 0.7. Future implementation of energy management strategies will see the use of the information on the engine's power limitation.

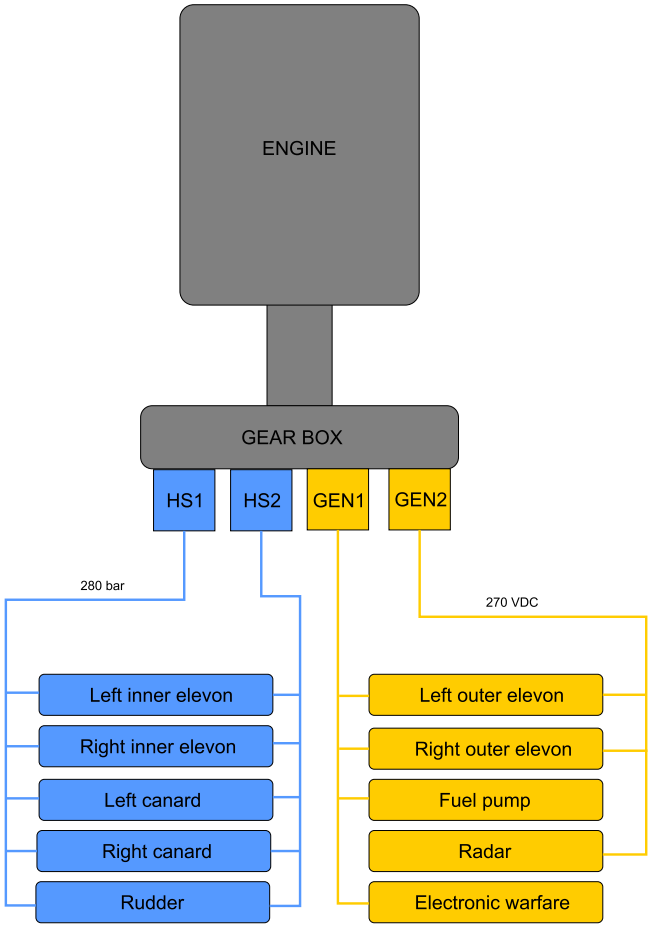

Figure 9 – On-board systems architecture for the case study.

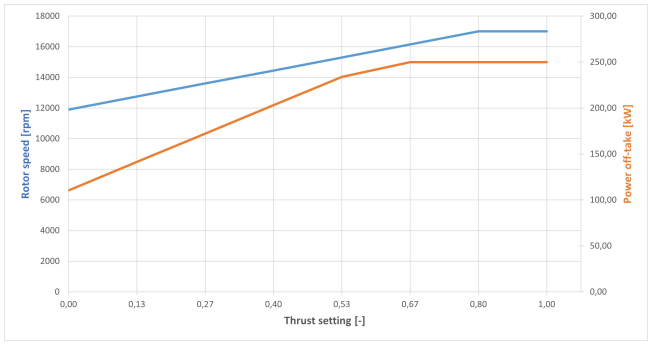

Figure 10 – Engine model providing shaft speed and max power off-take.

The fuel system consists of a boost pump that increase the fuel supply pressure when the after burner is activated. The maximum power is assumed to be 10 kW and is set to vary with the engine throttle setting. It is implemented as a pure resistive load with varying resistance depending on the power.

3.2.1 Electric power generation

The generator is represented by one single DC machine since only one unit is emulating the DC output in the rig. The generator model accounts for the back-emf and internal resistance. By using a DC equivalent model to the AC generator excludes any high frequency dynamics that would slow down the computational time. No dynamic characteristic is included since that is handled by the DC emulation units. The DC machine connects to the engine model's rotational speed port that is scaled through an ideal gearbox from a nominal value of 15000 rpm to 5000 rpm. The generator is set to give 270 VDC at 5000 rpm and varies with speed and load. A DC-DC converter regulates the output voltage to 270 VDC to the loads. The converter is a behavioral model that accounts for the droop

voltage at 1 % of nominal load and an efficiency, set to 97 %. The total input power to drive the generator is given from the torque and speed of the DC machine model. The implemented model is shown in figure 11.

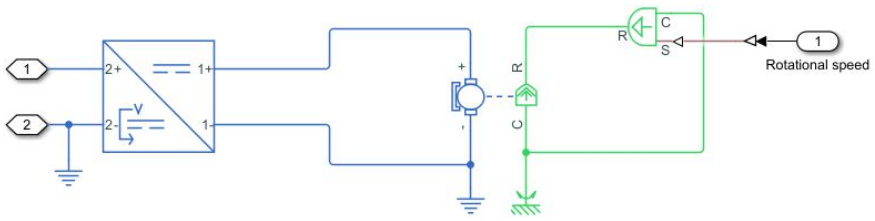

Figure 11 – The *Simscape* implementation of the electric power generation system.

3.2.2 Flight control actuation

The electromechanical actuator model takes advantage of the same approach as the electric power generation system by implementing a DC equivalent circuit. The governing equations are 1 to 4. A duplex machine is considered where the output torque, T_m, is proportional to the current, i, for each electric circuit. Only resistive losses are considered so the voltage across the machine is proportional to the rotational speed ω and the current. The machine also has a rotational inertia, J, and a viscous friction with coefficient B. T_L is an external torque that connects to the flight control surface.

$$U_1 = K_e\omega + Ri_1 \tag{1}$$
$$U_2 = K_e\omega + Ri_2 \tag{2}$$
$$T_m = K_t i_1 + K_t i_2 \tag{3}$$
$$J\dot{\omega} = T_m - B\omega + T_L \tag{4}$$

An inverter assumes a constant power and accounts for a constant efficiency, η, at 95 %. The supply current, i_{in}, is calculated by equation 5, where i_{out} and U_{out} are the electric motor's current and voltage, and U_{in} is the main supply voltage.

$$i_{in} = \frac{i_{out}U_{out}}{U_{in}\eta} \tag{5}$$

A speed control loop and a position control loop are implemented in a cascaded manner. Normally, a current control loop is also present but not included here to avoid high frequency dynamics that would slow down computational time. The speed control loop has a proportional-integral link in the path tuned to have a response time of 1 ms. The position control loop is strictly proportional with a time response of 5 ms.

The servohydraulic actuator model is implemented as a duplex cylinder and servo valve. No oil compressibility is included. Thus, there are four chambers where the output force equals the sum of each piston area's contribution from the exerted pressure as in equation 6. The piston area, A_p, are set equal for each chamber and are defined according to the actuator's stall load and supply pressure, p_s, according to equation 7. The tank pressure is assumed to be zero.

$$F = p_A A_p - p_B A_P + p_C A_P - p_D A_p \tag{6}$$
$$A_p = \frac{F_{stall}}{2p_s} \tag{7}$$

The servo valve, based on the *Simscape* 4-way directional valve component, includes all flow paths between the supply and tank ports and the cylinder chamber ports and accounts for the transition between laminar to turbulent flow. The maximum spool opening is based on the maximum flow, assuming it is turbulent, which is proportional to the cylinder speed and piston area. An additional

Segment	Altitude [km]	Speed	Turn	Radar mode	EW mode
Take-off	0.2	200 kts	-	10 %	10 %
Climb	to 10	5 km/s	-	10 %	10 %
In-bound	10	M 0.9	moderate turning	10 %	10 %
Ingress	10	M 1.2	-	10 %	10 %
Combat	dive to 5	M 1.2	hard turning	10 %	10 %
Egress	climb to 10	M 0.9	-	10 %	10 %
Outbound	10	M 0.7	-	10 %	10 %
Landing	Descend to 0.2	200 kts	-	10 %	10 %

Table 2 – Overview of the simulated mission and loads.

leakage curve is defined for each spool land, that is, between the supply pressure port and each chamber port, and between each chamber port and tank port. The maximum leakage occur when the spool is at center and gradually decays as the spool closes on that side. An example curve is shown i figure 12.

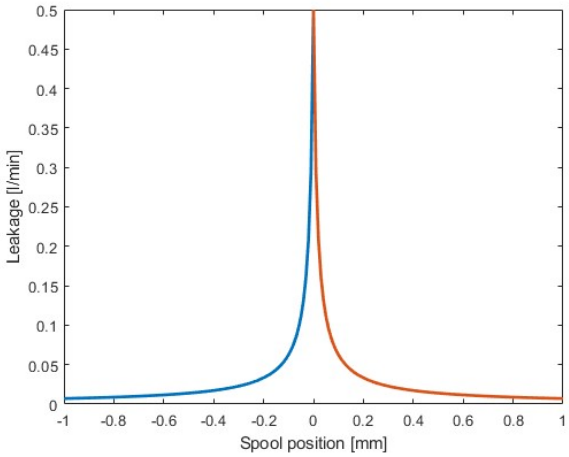

Figure 12 – The leakage curve with the blue showing from supply to chamber A and the red from supply to chamber B.

The controller is here strictly proportional tuned to get a first order response of 5 ms. The hydraulic supply system is simplified to an ideal constant pressure source at 280 bar.

3.2.3 Mission system

The two mission systems are modelled as a resistive load with variable resistance. The flight management system dictates the current mode for the radar and EW system depending on the mission segment. They are assumed to be a pure constant load with a fixed power consumption for each segment. The resistive load means that the current varies for changes in the supply voltage. The variable resistance is calculated from the power demand and a constant supply voltage of 270 VDC.

3.2.4 Mission configuration

The flight model is configured for the mission defined table 2. It is strictly fictive for illustration purposes. It consists of several different segments where the different loads and actuation system work in various manners.

An auto-pilot function is implemented to follow the defined mission. It consists of a guidance controller that control the pitch angle and roll angle. The controller has only a proportional link but the gain varies with the dynamic pressure to account for the changed aircraft response with altitude and speed. An altitude controller ensures that the altitude is maintained. It is a PD-controller with constant gains.

3.3 Implementation and testing

The virtual model of the aircraft and on-board systems are implemented in the real-time system and interfaced with the respective IO.

3.3.1 Scaling

The signals that control the hardware in the Iron Bird have to be scaled to matched to corresponding specifications. The electrical loads, radar, EW, and fuel pump, are scaled to match the maximum allowed current of the distribution system. The scaling is proportional to the maximum current of the virtual load and the physical allowed load.

The hinge moments are also scaled to match the physical actuators in the rig. The commanded control surface deflection is converted to a commanded actuator position through the hinge arm, 0.16 m and 0.08 m respectively for the EMA and the SHA. The measured actuator position is fed back through the scaling factor to calculate the hinge moments. These are scaled to match the maximum stall load of the actuators according to equation 8, where $F_{max,act}$ is the physical actuator's stall load, $F_{max,model}$ is the virtual model's stall load, and l_{hinge} is the hinge arm length. The scaled hinge moments are thus the commanded load for the air load system.

$$F_{cmd} = \frac{1}{l_{hinge}} \frac{F_{max,act}}{F_{max,model}} \tag{8}$$

3.3.2 Results

The results from the simulation in the Iron Bird are shown in figures 13 and 14. A subset of the flight mission is shown to highlight the behaviour. The first plot shows the air load system performance during a massive manoeuvre for the left wing EMA. Both the actuator movement and corresponding load is shown with good performance of the air load system. Figure 14 shows the emulated electrical loads for the fuel pump, radar, and EW system, as the scaled current. Both the reference current from the virtual model and the current draw in the Iron Bird are shown. The electrical emulation system manage to follow the intended behaviour.

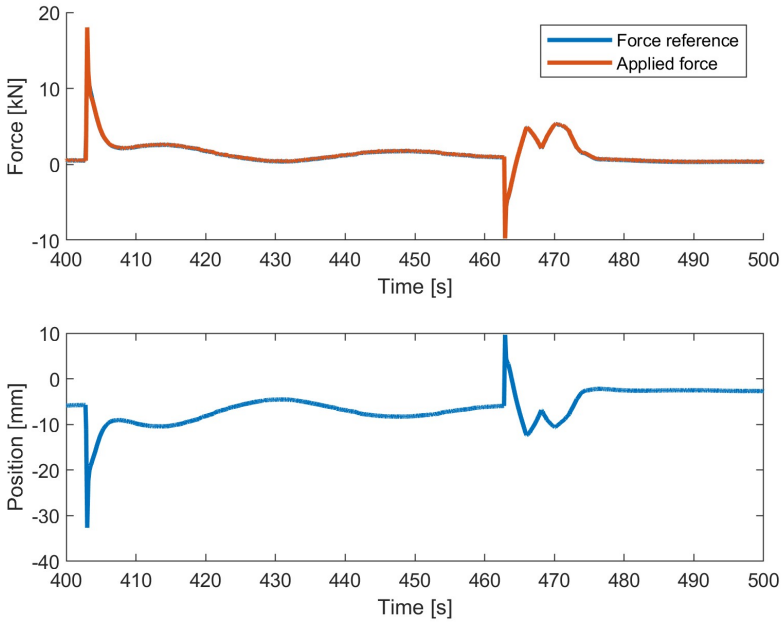

Figure 13 – The performance of the implemented air load system. The top figure showing the reference and applied load, the bottom showing the EMA movement.

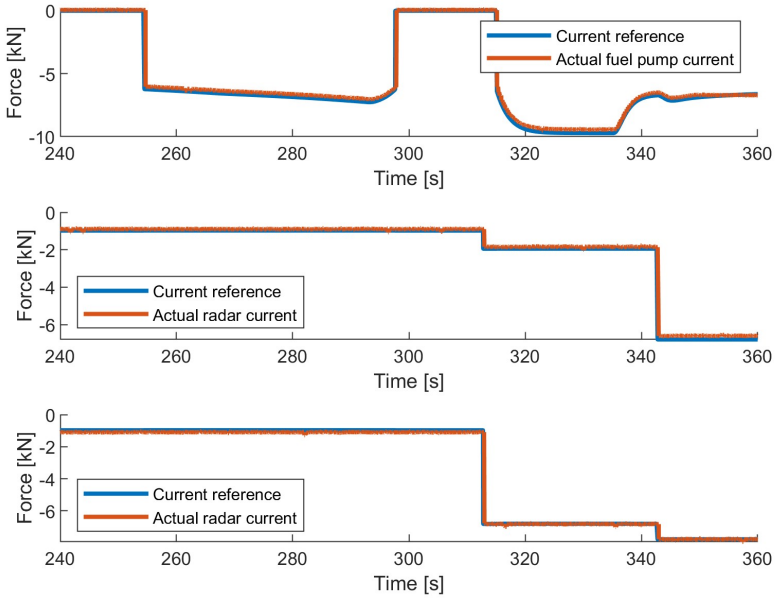

Figure 14 – Results from the load emulation system showing the three implemented electric loads: fuel pump, radar, EW system.

4. Conclusions

This paper has demonstrated the Iron Bird under development at Linköping University, a test rig for energy management research studies. Electric and hydraulic actuation, electric and hydraulic supply and distribution, and electric load emulation are integrated to form a hardware-in-the-loop simulation platform. A virtual model of the intended aircraft is developed and implemented in the real-time system. The Iron Bird is capable of a complete flight mission simulation, which has been demonstrated through a case study of a generic fighter aircraft and an on-board systems architecture.

5. Acknowledgement

The author want to acknowledge the contribution from the thesis work in [18], [19], [20], and [21] on the implementation of several control and communication features in the Iron Bird.

6. Contact Author Email Address

alessandro.dellamico@liu.se

7. Copyright Statement

References

[1] Miguel A. Maldonado, Naren M. Shah, and Keith J. Cleek. Power management and distribution system more-electric aircraft (madmel). *IEEEAES Systems Magazine*, 1999.

[2] Giampaolo Buticchi, Pat Wheeler, and Dushan Boroyevich. The more-electric aircraft and beyond. *Proceedings of the IEEE*, 111(4), 2023.

[3] A. A. AbdElhafez and A. J. Forsyth. A review of more-electric aircraft. In *13th International Conference on AEROSPACE SCIENCES & AVIATION TECHNOLOGY*, 2009.

[4] Daniel Schlabe and Jens Lienig. Energy management of aircraft electrical systems - state of the art and further directions. In *Electrical Systems for Aircraft, Railway and Ship Propulsion*, 2012.

[5] 11. S Liscouët-Hanke, S Pufe, and J-CMaré. A simulation framework for aircraft power management. *the Institution of Mechanical Engineers, Part G: Journal of Aerospace Engineering*, 222(6):749–756, 2008.

[6] A. Cavallo and and B. Guida G. Canciello. Energy storage system control for energy management in advanced aeronautic applications. *Mathematical Problems in Engineering*, 2017.

[7] R. Todd, D. Wu, J.A. dos Santos Girio, and A.J. Forsyth M. Pouc and. Supercapacitor-based energy management for future aircraft systems. In *Twenty-Fifth Annual IEEE Applied Power Electronics Conference*, 2010.

[8] Torben Schroeter and Detlef Schulz. An approach for the mathematical description of aircraft electrical systems' load characteristics including electrical dependences validation. In *Electrical Systems for Aircraft, Railway and Ship Propulsion*, 2010.

[9] T. Gerkens, G. Fritsch, C. Seyffert, J. Büttner, and I. Morrish I. Mugtussidis. The iron bird for the fairchild-dornier 728. *Aerospace Science and Technology*, 8:231–243, 2004.

[10] Dawei Li, Mingxing Lin, and Liang Tian. Design of iron bird for a regional jet aircraft. *Proceedings of the Institution of Mechanical Engineers, Part I: Journal of Systems and Control Engineering*, 2019.

[11] Blasi L., Borrelli M., D'Amato E., di Grazia L.E., Mattei M., and Notaro I. Modeling and control of a modular iron bird. *Aerospace*, 8(39), 2021.

[12] Jean-Charles Maré and Jian Fu. Reivew on signal-by-wire and power-by-wire actuation for more electric aircraft. *Chinese journal of aeronautics*, 30(3):857–870, 2017.

[13] Felix Larsson. *Evaluation of Aircraft Actuator Technologies*. Linköping University Electronic Press, 2023.

[14] J-C Maré. Dynamic loading systems for ground testing of high speed aerospace actuators. *Aircraft Engineering and Aerospace Technology: An International Journal*, 78(4):275–282, 2006.

[15] G. Jacazio and G. Balossini. Real-time loading actuator control for an advanced aerospace test rig. *Proceedings of the Institution of Mechanical Engineers, Part I: Journal of Systems and Control Engineering*, 2007.

[16] Alessandro Dell'Amico. Design and implementation of an ema iron bird air load simulation system. In *Recent advances in aerospace actuation systems and components*, 2023.

[17] Lars Forsell and Ulrik Nilsson. Admire the aero-data model in a research environment version 4.0, odel description. Technical Report FOI-R–1624–SE, FOI – Swedish Defence Research Agency, Systems Technology, 2005.

[18] Max Lundström and Johannes Wenngren. More electric aircraft power system for real-time hardware-inthe-loop simulation. Master's thesis, Linköping University, 2022. LIU-IEI-TEK-A–22/04397–SE.

[19] David Andersson and Isac Lundin. Evaluation of aircraft future electric power system. Master's thesis, Linköping University, 2023. IU-IEI-TEK-A–23/04624—SE.

[20] Anton Gustafsson and Jacob Ludewig. Assessment and hardware-in-the-loop simulations of power management control strategies for future fighter aircraft, master's thesis. Master's thesis, Linköping University, 2023. IEI-TEK-A–23/04645—SE.

[21] Anton Nygårds and Dennis Moliner Pettersson. Evaluation of electric actuation for fighter aircraft. Master's thesis, Linköping University, 2023. LIU-IEI-TEK-A–23/04681–SE.